Electronic Supplementary Material (ESI) for Lab on a Chip.

Supplementary Information

Transportation, Dispersion and Ordering of Dense Colloidal Assemblies by Magnetic Interfacial Rotaphoresis

*Alexander van Reenen, Arthur M. de Jong, and Menno W.J. Prins**

Contents:

A. Interfacial rotaphoresis experiments

Interfacial rotaphoresis was studied in experiments using different types of superparamagnetic particles. In most experiments, ∅2.8 μm carboxyl M270 particles (Dynal Biotech) were used. In addition, we studied interfacial rotaphoresis with: ∅2.8 μm streptavidin-coated M270 particles (Dynal Biotech); ∅2.6 μm carboxyl Micromer particles (Micromod); ∅1.0 μm carboxyl and streptavidin-coated MyOne particles (Dynal Biotech); and ∅500 nm carboxyl and streptavidin-coated MasterBeads (Ademtech). Unless otherwise stated, particles were suspended in undiluted phosphate buffered saline containing 0.1% bovine serum albumin (BSA; Merck) and 0.02% Tween-20 (Thermo Scientific). Alternatively, particles were spiked in undiluted fetal bovine serum (Thermo Scientific).

Particle suspensions (diluted to ~0.5 mg/mL) were pipetted in 38 μL fluid chambers, assembled by attaching adhesive Secure-Seal™ Hybridization chambers (∅9 mm, height = 0.6 mm; Electron Microscopy Sciences) to a glass cover slip (22×22 mm^2 from VWR) that was cleaned beforehand using isopropanol. On the non-adhesive side, the Hybridization chambers contained a 0.25 mm thick and transparent polycarbonate sheet containing two inlets to fill the 38 μL incubation chamber. The fluid chamber was imaged from this side with a Leica DM6000 microscope. Prior to an experiment, the incubation chamber was filled with assay buffer without particles for 30 minutes to block the chamber walls with BSA in order to prevent non-specific adhesion of the particles to the surfaces. After that, the assay buffer was removed from the fluid chamber and the chamber was filled with the particle suspension. The fluid chamber was sealed using adhesive port seals as supplied together with the Hybridization chambers.

To apply magnetic fields to the suspended particles, the fluid chamber was placed in a custom-build 5-pole electromagnet setup as shown in Figure 1b and Figure S1. Briefly, it consists of a quadrupole electromagnet (800 windings with ∅0.25 mm copper wires) to generate horizontal magnetic fields at the position of the fluid chamber (see Figure S1a,c). In addition, a separate electromagnet (1600 windings with ∅0.25 mm copper wires) is positioned below the center of the quadrupole electromagnet to allow for the generation of vertical fields. Using the quadrupole electromagnet, magnetic fields can be generated that rotate in-plane with respect to the bottom surface of the fluid chamber. By combining the bottom electromagnet with two opposite electromagnets of the quadrupole, magnetic fields can be generated that rotate out-of-plane. To enhance the field line density within the incubation chamber, soft iron parts were implemented in the setup.

The electromagnets were powered separately using a LabView-steered controller based on prescribed protocols of the separate currents which could be varied in time in terms of the amplitude, frequency and shape (i.e. sinusoidal). The magnetic field was calibrated using a Gauss meter (5100 series F.W. Bell) and corresponding data is shown in Figure S2. Details of the exact actuation protocol that was applied to obtain interfacial rotaphoresis are given in Supplementary Information C.

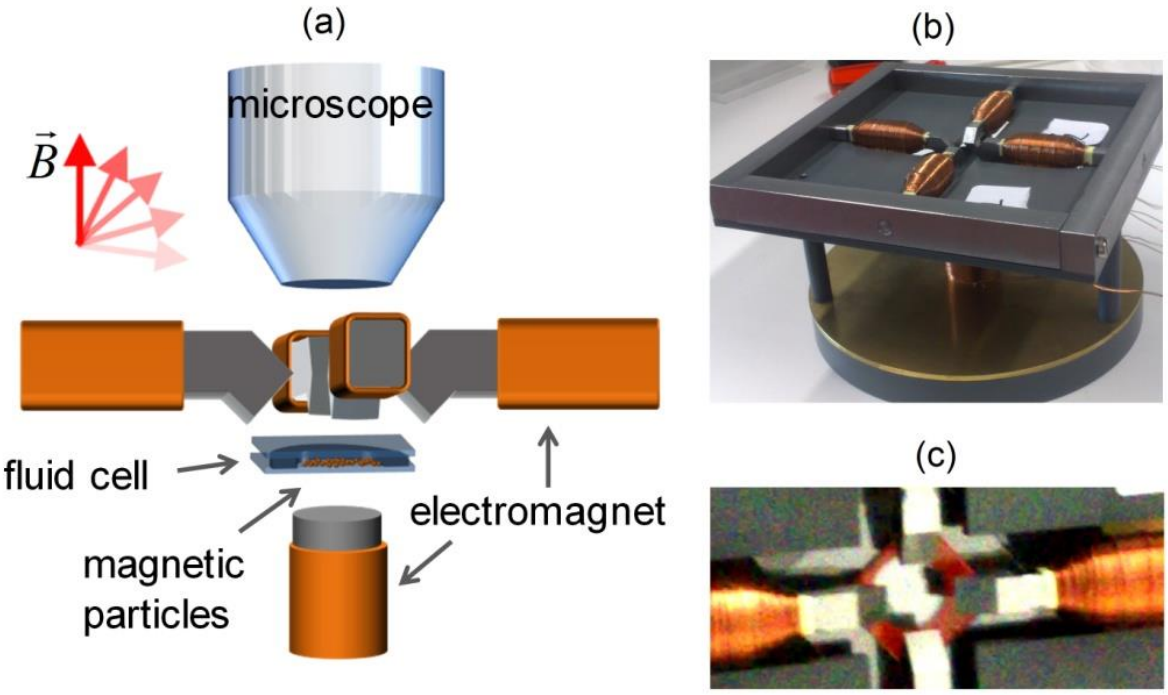

Figure S1. 5-pole electromagnet. A 5-pole electromagnet was used to apply fields in all directions. The setup consists of a quadrupole electromagnet and a separate electromagnet oriented orthogonal with respect to the center of the quadrupole. (a) Schematic drawing of the center of the setup, indicating the position of the magnets and the microscope with respect to the fluid cell. (b) Picture of the 5-pole electromagnet system. The quadrupole electromagnets are connected via a soft-iron yoke, to guide the field lines. (c) Picture of the fluid cell positioned within the center of the 5-pole electromagnet (compare to panel a).

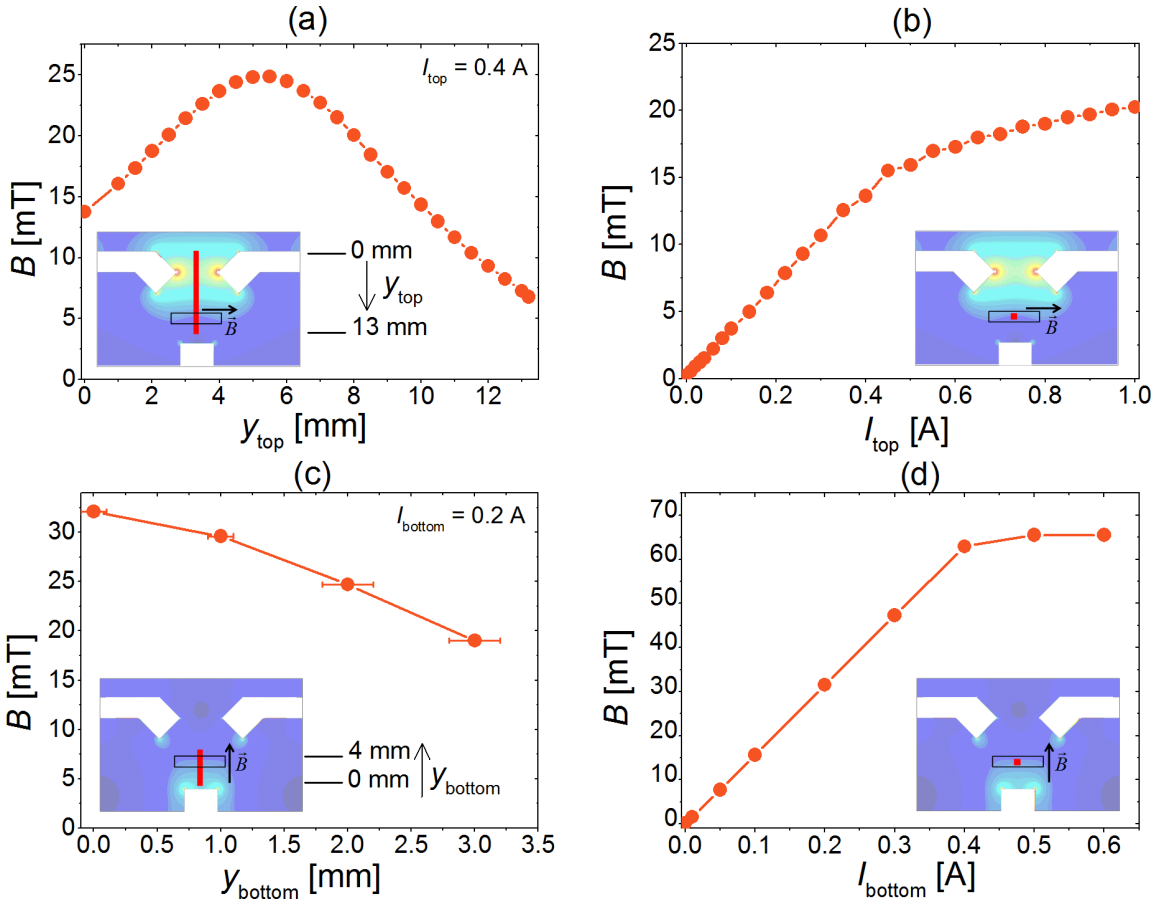

Figure S2. Calibration data of the 5-pole electromagnet. Field calibration data of the 5-pole electromagnet measured using a Gauss meter (F.W. Bell). In each calibration figure the inset shows a cross-section of the electromagnets (showing two top magnets and the bottom magnet). The cross-sectional views show the position (red rectangles) and the component (black arrows) of the measured field. The location of the incubation chamber is indicated by the black open rectangle. In the background of the cross-sectional views, the (relative) field strength is plotted (following a heat color map) as obtained from simulations using Comsol Multiphysics. The following field calibrations are shown in the different panels: (a) In-plane field dependence of the distance from the top magnets, y_{top}, for the case two opposite top magnets are powered in series at I_{top} = 0.4 A. (b) The in-plane field dependence to the current I_{top} at the position of the incubation chamber, for the case two opposite top magnets are powered in series. (c) Dependence of the out-of-plane field to the distance from the bottom magnet, y_{bottom}, for the case that only the bottom magnet is powered at I_{bottom} = 0.2 A. (d) Dependence of the out-of-plane field to the current I_{bottom} at the position of the incubation chamber, for the case that only the bottom magnet is powered.

B. Interfacial rotaphoresis for different types of particles

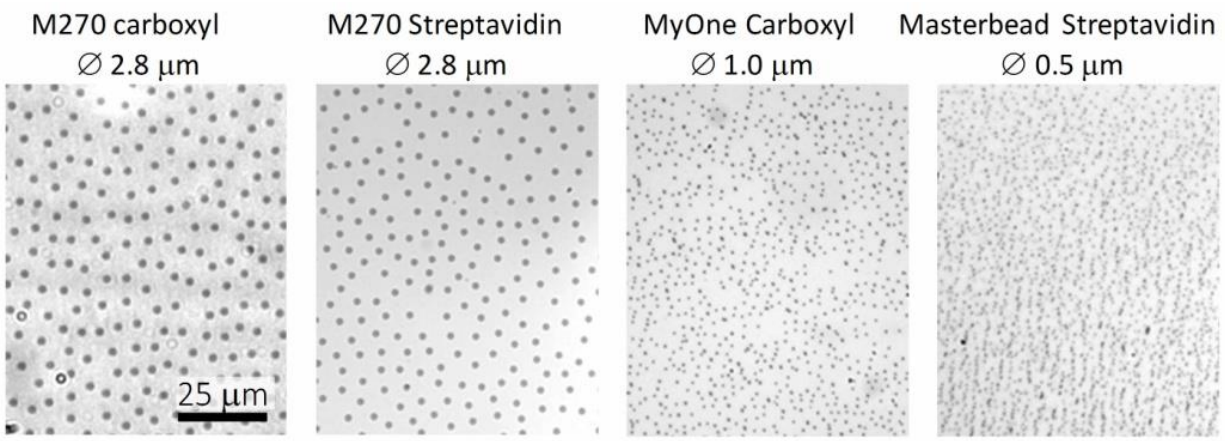

Figure S3. Microscope images of magnetic particle distributions after interfacial rotaphoresis for different types or functionalizations of particles. The details for the different cases are shown above each figure. Particles were suspended in PBS containing 0.1% BSA and 0.02% Tween-20. Also see Supplementary Videos 1, 6 and 7 for respectively M270 carboxyl particles in PBS containing 0.1% BSA and 0.02% Tween-20; MyOne Streptavidin particles in PBS containing 0.1% BSA and 0.02% Tween-20; and protein G-coated M270 carboxyl particles spiked in fetal bovine serum.

Table S1. Overview of interfacial rotaphoresis applied to different types of particles. In all cases, applied weight percentages of magnetic particles were 0.3 mg/mL. Information on the particle size and magnetic properties were obtained either from the suppliers or from scientific literature[37]. The maximum induced velocity was obtained in a similar way as results in Figure 2d-f for particle concentrations of ~0.5 mg/mL.

Particle type	Particle diameter [μm]	Surface functionalization	Saturation magnetization [emu/g]	Maximum induced velocity [mm/s]	Disaggregation observed
Dynal M270	2.8 ± 0.1	Carboxylic acid	7.1 ± 0.5	3.0 ± 0.2	Yes
		Streptavidin		2.6 ± 0.2	Yes
		Protein G		2.7 ± 0.3	Yes
Micromod Micromer	2.6 ± 0.1	Carboxylic acid	2.6 ± 0.4	2.6 ± 0.2	Yes
Dynal MyOne	0.99 ± 0.04	Carboxylic acid	13 ± 0.1	4.0 ± 0.3	Yes
		Streptavidin		3.8 ± 0.3	Yes
Ademtech Masterbead	0.5 ± 0.1	Carboxylic acid	40 ± 5	2.7 ± 0.2	Yes
		Streptavidin		2.6 ± 0.3	Yes

C. Particle behavior for different rotaphoretic field configurations

To induce interfacial rotaphoresis, a straightforward field configuration is the application of a rotating field with a constant field amplitude and the normal vector of the plane of rotation parallel to the surface. However, the rotating field does not necessarily need to be constant, and the normal vector of the plane of rotation can also have a component along the surface normal. Therefore, we have studied the behavior of magnetic particles for different rotaphoretic field protocols, both in experiments and in numerical simulations. Specifically, we studied three different rotaphoretic field configurations (see Figure S4). The functional form of the modelled magnetic field was:

$$\vec{B}(t) = \begin{bmatrix} \vec{B}_x(t) \\ \vec{B}_y(t) \\ \vec{B}_z(t) \end{bmatrix} = \begin{bmatrix} B_x \cos(2\pi f_x t)\hat{e}_x \\ B_y \sin(2\pi f_{zy} t)\hat{e}_y \\ B_z \cos(2\pi f_{zy} t)\hat{e}_z \end{bmatrix}. \quad \text{(S.4)}$$

Basically, the fields in the *y*- and *z*-direction constitute the basic rotaphoretic field, governed by the frequency f_{zy}. The field component in the *x*-direction was added to enable actuation in three dimensions (see Figure S4c).

First, in case a constant magnetic field is applied that rotates about the *x*-axis, it was observed that particles formed into large linearly shaped aggregates that move over the surface (Figure S4a; also see Supplementary Video 8). Due to the large size, the formed aggregates did not show any visible rotational response to the rotating field. From these results, we conclude that this interfacial rotaphoresis protocol allows displacing particles over the surface, but the particles are not redistributed and rather form large multi-particle clusters.

Based on an approach reported by Gao et al.[45], a second interfacial rotaphoresis protocol was tested with an out-of-plane component of the rotating field, B_z, that is larger than the in-plane field component, B_x. After the application of the in-plane field B_x (orienting clusters parallel to the surface), the stronger out-of-plane field B_z induces repulsive magnetic dipole-dipole interactions between the particles. While disaggregation of clusters was observed for small particle clusters (see simulation results in Figure S4b and Supplementary Video 9), for high local particle concentrations the particles remained ordered as long chains, as disaggregated particles tended to stay in the plane of the rotating cluster and did not sufficiently separate to prevent re-aggregation. As a result, no effective particle redistribution is obtained for this field configuration.

To better spread out disaggregated particles over the surface, a rotaphoretic field was tested with field components in three dimensions instead of two. This was achieved by superimposing the rotating field with an alternating field parallel to the axis of rotation, i.e. along B_y. For example, when the out-of-plane rotating field is generated by the north and south electromagnet of the quadrupole (Figure S1) and the electromagnet below the fluid chamber, the east and west magnet are also powered using a smaller current and at a lower frequency. This causes the rotating field to change its direction over time: the normal vector of the plane of rotation has a component that is parallel to the surface and a time-dependent component along the surface normal, i.e., the field shows rotation combined with a wiggling motion orthogonal to the rotation

direction. As shown in Figure S4c and in Supplementary Video 3, this rotaphoretic field caused particle clusters to completely disaggregate, and evenly redistributed particles over the surface.

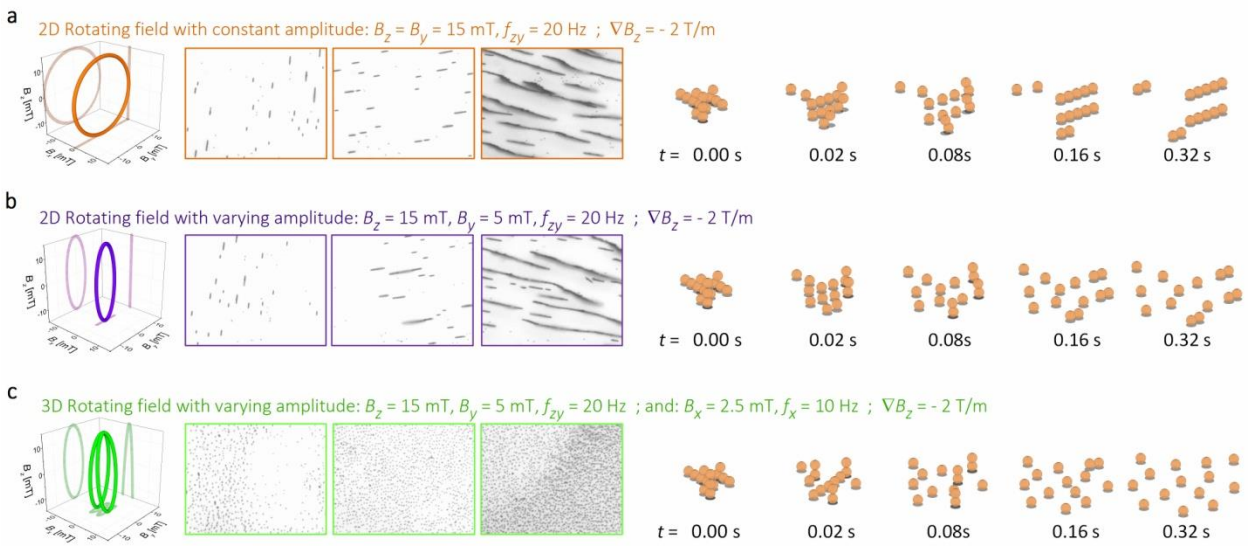

Figure S4. Response of magnetic particles to different rotaphoretic field configurations. Data from experiments and numerical simulations on 2.8 μm Dynal M-270 particles. The different field configurations are (see the left panels) (a) a constant rotating field about the *x*-axis; (b) a rotating field about the *x*-axis with a larger amplitude of the out-of-plane component, B_z, compared to the in-plane component, B_x; and (c) a rotating field with similarly varying amplitude, superimposed with an alternating field component orthogonal to the rotating field, i.e. along B_y. For all cases, a field gradient of 2 T/m was applied directed towards the surface, i.e. in the –*z*-direction. In the center part of the figure, top-view microscope images are shown at different particle densities during interfacial rotaphoresis. On the right, the effect of the different rotaphoretic protocols is shown in numerical simulations of 14-particle clusters.

D. Estimation of the ratio of torques in interfacial rotaphoresis

We estimated the relative contributions of the hydrodynamic drag and magnetic torque acting on a chain of magnetic particles rotating near a surface.

For a chain of particles rotating in an unbounded bulk fluid (i.e. without a nearby surface), Gao et al.[34] described a detailed expression for the dimensionless Mason number to estimate the ratio between hydrodynamic versus magnetic torques:

$$\mathrm{R_T} = 16\frac{\eta\omega}{\mu_0\chi_p^2 H_0^2}\frac{N^3}{\left(\mathrm{N}-1\right)\left(\ln\left(\frac{N}{2}\right)+\frac{2A}{N}\right)}. \qquad \text{(S.1)}$$

Here η is the viscosity of the medium, N is the number of particles within the chain, μ_0 the permeability of free space and χ_p the particle susceptibility. Essentially, in case $R_T < 1$ chains do not break, whereas in case $R_T > 1$ chains show infinitely repeating break-and-reformation behaviour.

In this Section, we estimate whether rotating chains will break up or remain rigid when they are colliding with a solid interface. The influence of the nearby surface is taken into account by an additional viscous drag on the particles due to the no-slip boundary. As explained in the methods section, the experiments were performed in a phosphate buffer ($\eta_{PBS} = 10^{-3}$ Pa·s). Considering the rotating magnetic field, we applied a field with an average strength of 10 mT and a rotation frequency of 20 Hz. At this field strength, the used particles have a magnetic moment of $m = (6.0 \pm 0.3) \times 10^{-14}$ A·m^2 as characterized in previous work[37] using a method called intra-pair magnetophoresis. From this work, it was found that the used magnetic particles already show some saturation in the magnetization at field strengths of 10 mT.

Using these parameters, we estimate the ratio of torques both for a particle chain in the bulk and a particle chain near a surface (see Figure S5). Effectively, the nearby surface enhances the hydrodynamic drag on the particle chain. For a particle that is half its radius away from the surface, the hydrodynamic drag on the particle increases[48] by a factor of ~4. Assuming this value as an approximation of the effective viscosity experienced by the whole particle chain, we find in Figure S5 that (i) when near the surface, all particle chains will demonstrate breaking-behavior, whereas (ii), when in the bulk, chains with lengths of less than 4 particles will not break.

In particular, when a chain rotates near a surface, the particle colliding with the surface will experience a high drag force compared to the other particles. This is due to the hydrodynamic no-slip boundary condition, but also due to normal forces resulting from the hard-sphere collision with the surface. To maintain the rotation, the particle chain has to erect from the surface and rotate about the colliding particle. Effectively, the forces acting on the chain are comparable to the forces on a chain with an increased length (i.e., if the enhanced drag forces due to the nearby surface are neglected). More precisely, the axis of rotation shifts from the center of mass of the chain (with length N) to the center of the colliding particle. Correspondingly, the forces acting on the other end of the particle chain become comparable to a freely rotating chain with length $2N - 1$. So, when a chain of $N = 3$ collides with the surface, the ratio of torques becomes comparable to a chain with a length of $N_{eff} = 2N - 1 = 5$. Neglecting the enhanced drag due to the surface, such a chain (i.e., $N = 5$) will break up, while the original chain

(i.e., $N = 3$) will not break up in the bulk fluid (see Figure S5). Taking into account the enhanced drag, also for a two-particle chain it is expected that a collision with the surface will break the chain, whereas in the bulk fluid, this does not occur as $R_T < 1$ in that case.

Based on these considerations, the given configuration of magnetic and hydrodynamic forces should result both in the translation and gradual disaggregation of a particle chain that rotates in the vicinity of a physical boundary.

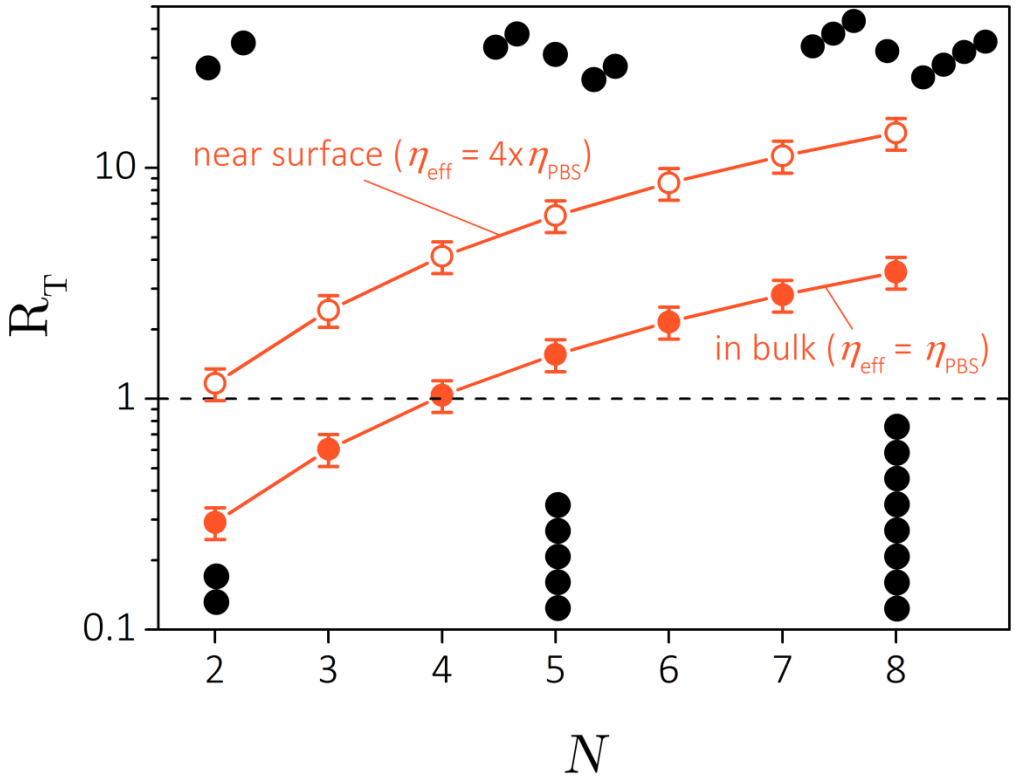

Figure S5. Estimated ratio of hydrodynamic vs magnetic torques for rotating particle chains consisting of N particles in the bulk and near a surface. The computed errors in R_T are composed of the relative error in the magnetic moment (~5%) and the applied field strengths (< 10%).

E. Experiments on particle-based capture of antibodies from a fluid

The capture of targets from a fluid by magnetically actuated magnetic particles was studied using a model system comprising protein G-coated M270 particles which captured goat anti-mouse IgG antibodies labeled with fluorescent dye molecules (Alexa fluor® 488 dye; Invitrogen). The magnetic particles were coated with recombinant protein G (Thermo Scientific) using standard EDC-NHS coupling chemistry.

Experiments were conducted using the same fluid chambers as used in the interfacial rotaphoresis experiments. First, the fluid chambers were blocked by incubating 1 mg/mL BSA for 10 minutes. Subsequently, a 4 μL magnetic particle suspension (4×10^5 particles/μL) was inserted by means of a pipette. During one minute, the particles were allowed to sediment to the bottom surface. Thereafter the fluid chamber was filled with the target solution (~34 μL and diluted to 110 pM). The fluid chamber was closed and either placed in the center of the 5-pole electromagnet (see Figure S1) to actuate the particles, or under the microscope to measure the fluorescence. The incubation process was studied without magnetic actuation and with magnetic actuation. In the latter case, a repeated sequence was applied of rotating fields for target capture (500 s) and interfacial rotaphoresis to redisperse particles over the surface (80 s). The actuation for target capture consists of a continuously rotating magnetic field (20 mT, 0.2 Hz) rotating in-plane with the surface (i.e. rotating about the *z*-axis), combined with field gradients (4 T/m) to move particles up and down through the fluid chamber (i.e. along the z-axis).

To measure the particle fluorescence, excitation light (λ = 480 ± 20 nm) was generated by an external light source (Leica EL6000) combined with a L5 (Leica) filter cube. Fluorescence (within the range of λ = 527±15 nm) was recorded using an EMCCD camera (Andor Luca S). For each measurement, images were taken from three random locations (with a field of view of 142×107 μm^2).

Images (e.g. Figure 3d) were processed using ImageJ software (http://rsbweb.nih.gov/ij/) and Matlab (Mathworks) to determine the average fluorescence intensity of the particles with respect to the background intensity. First, a binary image was made using a threshold to determine the area occupied by the magnetic particles. Subsequently Matlab software was used to determine the average intensity of the pixels corresponding to the particles or the background. As the intensity is averaged over the number of pixels, a single measurement is independent of the number of particles within a single field of view.

To verify the specificity of the experimental model system, control experiments were conducted, in which the incubation was performed under turbulent mixing using a vortex mixer, as shown in Figure S6.

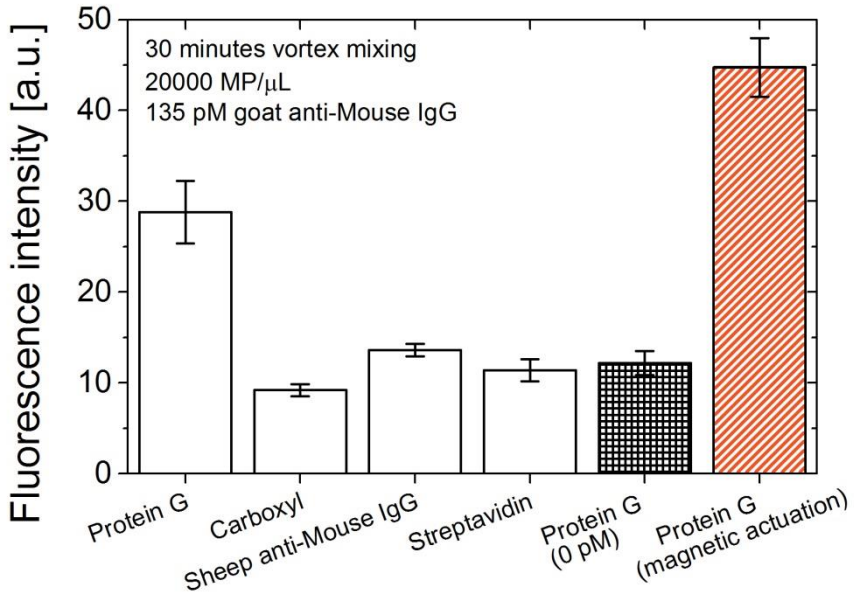

Figure S6. Control experiments for the specificity of the experimental model system: goat anti-mouse IgG and protein G-coated magnetic particles. The average particle fluorescence was measured after 30 minutes of incubation of the reagents on a vortex mixer, except for the orange bar. Different surface functionalizations were tested: protein G; carboxyl (hydrophilic); sheep anti-mouse IgG and streptavidin. To determine the contribution to the fluorescence intensity due to the auto-fluorescence of the magnetic particles, a measurement was performed with a zero target concentration (i.e. the black bar). The error bars correspond to the standard deviation in the determined fluorescence intensity.

F. Supplementary Videos

Supplementary Video 1: Disaggregation of small particle assemblies

The disaggregation of small particle clusters by interfacial rotaphoresis with field components in three dimensions, corresponding to Figure 1c. The used particles were ∅2.8 μm, Dynal M270 particles. The video shows that two-particle clusters rotate several times before finally disaggregating. Specifically, the applied rotaphoretic field consists of a field rotating out-of-plane at 20 Hz with an in-plane component B_x of 5 mT and an out-of-plane component B_z of 15 mT; and additionally an orthogonal field B_y of 2.5 mT with a sinusoidal shape (10 Hz). The total duration of the movie is about 2 seconds.

Supplementary Video 2: Simulation of a 40-particle cluster with 3D interfacial rotaphoresis

Simulated response of a 40-particle cluster to a rotaphoretic field with components in three dimensions. The simulated 3D rotaphoretic field consists of a field rotating out-of-plane at 20 Hz with an in-plane component B_x of 5 mT and an out-of-plane component B_z of 15 mT; and additionally an orthogonal field B_y of 2.5 mT with a sinusoidal shape (10 Hz). The particles in the numerical model correspond to ∅2.8 μm, Dynal M270 particles. It is observed that large clusters displace faster than small clusters, and that the particle cluster disaggregates almost completely. Note that the disaggregated particles spread out over the surface into all directions.

Supplementary Video 3: Interfacial rotaphoresis by three-dimensional actuation

This video shows the response of magnetic particles (∅2.8 μm carboxyl Dynal M270) to a rotaphoretic field with components in three dimensions, corresponding to Figure 2a. Shown is a top-view of the west side of the fluid chamber. The particles start out aggregated as a large particle cluster near the electromagnet positioned west of the fluid chamber. A rotaphoretic field is applied consisting of a field rotating out-of-plane at 20 Hz with an in-plane component B_x of 5 mT and an out-of-plane component B_z of 15 mT; additionally we applied an orthogonal field B_y of 2.5 mT with a sinusoidal shape (with 10 Hz) to orient the field in the third dimension. The rotaphoretic field is applied to move particles to the magnet pole on the north side of the fluid chamber, so the particles are moving to the northeast. Subsequently the field direction is changed to move particles towards the east magnet pole, and lastly it is changed to move particles towards the south magnet pole. The particle behavior induced by this rotaphoretic field is substantially different than the behavior found in Supplementary Video 8, where the rotaphoretic field does not include a field component orthogonal to the rotating field.

Supplementary Video 4: Velocity induced by 3D interfacial rotaphoresis

This video contains the recorded images corresponding to the data in Figure 2d-e. Interfacial rotaphoresis is applied to a concentrated pack of particles with a diameter of ~1.5 mm. The maximum attained velocity is ~3 mm/s. The applied rotaphoretic field consists of a field rotating out-of-plane at 20 Hz with an in-plane component B_x of 5 mT and an out-of-plane component B_z of 15 mT; and additionally an orthogonal field B_y of 2.5 mT with a sinusoidal shape (10 Hz).

Supplementary Video 5: Field-induced aggregation and drift of particles

Recorded response of an initially homogeneous distribution of particles on the bottom surface of the fluid chamber to a magnetic field rotating in-plane with respect to the surface. The used field strength is B = 6 mT and the rotation frequency was f = 0.1 Hz. Images were recorded at the center of the incubation chamber at a frame rate of 0.1 Hz, such that the drift and the clustering becomes more clearly visible, in contrast to the rotation behavior which cannot be seen in the video. The video shows 15 minutes of the experiment.

Supplementary Video 6: Redistribution of 1 μm-sized particles

This video shows the application of a 3D interfacial rotaphoresis protocol to redistribute a cluster of 1 μm sized particles (carboxyl Dynal MyOne) over the surface. Initially, the particles are aggregated as a large cluster with a size of ~1 mm. Interfacial rotaphoresis is applied in different directions (east, south, west, and north and so on) with durations of 20 s per direction. Besides observing complete redistribution of the particles, interesting magnetorheological behavior of the particles over the surface is observed when the interfacial rotaphoresis direction is switched, especially when one particle layer crosses another. The video additionally shows that interfacial rotaphoresis is almost not affected by air bubbles or other material within the fluid cell. The applied rotaphoretic field consists of a field rotating out-of-plane at 20 Hz with an in-plane component B_x of 5 mT and an out-of-plane component B_z of 15 mT; and additionally an orthogonal field B_y of 2.5 mT with a sinusoidal shape (10 Hz).

Supplementary Video 7: Interfacial rotaphoresis of protein G-coated particles in fetal bovine serum

In this video, a 3D interfacial rotaphoresis protocol is applied to protein G-coated magnetic particles (∅2.8 μm Dynal M270) spiked in undiluted fetal bovine serum (FBS). Initially, the particles are concentrated manually using a ferromagnet near the electromagnet positioned on the south-side of the fluid chamber. The experiment was conducted at room temperature (T = 293 K). The video shows a similar particle response as in other videos, although a small amount of clusters remains, indicating the enhancement in non-specific adhesion due to the bio-functionalized particle surfaces in combination with the biological fluid. The applied rotaphoretic field consists of a field rotating out-of-plane at 16 Hz with an in-plane component B_x of 5 mT and an out-of-plane component B_z of 15 mT; and additionally an orthogonal field B_y of 2.5 mT with a sinusoidal shape (5 Hz).

Supplementary Video 8: Interfacial rotaphoresis by two-dimensional actuation

This video shows the response of magnetic particles (∅2.8 μm carboxyl Dynal M270) to a rotaphoretic field with components in two dimensions. The video (10 frames per second) shows a top-view of the west side of the fluid chamber. At the beginning of the video, the particles are aggregated into a large particle cluster and are close to the electromagnet west of the fluid chamber (< 1 mm). A rotaphoretic field is applied consisting of a magnetic field rotating out-of-plane at 20 Hz with an in-plane component B_x of 5 mT and an out-of-plane component B_z of 15 mT (and B_y = 0). In the first part of the video, the rotaphoretic field is applied to move particles to the magnetic pole on the south side of the fluid chamber. So the in-

plane field components are in the north-south direction. In the video, it is observed that the particle clusters split up in chain-like linear clusters (aligned with the in-plane magnetic field component B_x) and move towards the electromagnet on the south side of the fluid chamber at velocities of almost 1 mm/s. At 10 s in the video, the rotaphoretic field is switched to move particles to the magnetic pole on the east side of the fluid chamber (i.e. the in-plane field is now in the east-west direction). This field is found to split up the larger particle chains into smaller particle chains, which start moving to the east side of the fluid chamber. Note that the smaller chains show out-of-plane rotation, in contrast to the behavior of the larger chains earlier in the video. It is observed however that the smaller particle chains re-group with each other into larger chains again, and thus remain aggregated.

Supplementary Video 9: Simulation of a 40-particle cluster with 2D interfacial rotaphoresis

The simulated response of a 40-particle cluster to interfacial rotaphoresis with field components in two dimensions. Simulated particles correspond to ∅2.8 μm Dynal M270 particles. Similar behavior is observed as in Supplementary Video 8, but now disaggregated particles roughly end up on the same line behind the moving particle clusters. Similar behavior is also observed in experiments, e.g., see Supplementary Video 10. The simulated 2D rotaphoretic field consists of a field rotating out-of-plane at 20 Hz with an in-plane component B_x of 5 mT and an out-of-plane component B_z of 15 mT.

Supplementary Video 10: 2D interfacial rotaphoresis on smaller clusters

This video shows the response of particle clusters consisting of several tens of particles (∅2.8 μm carboxyl Dynal M270) to a rotaphoretic field with components in two dimensions on smaller clusters of particles. Similarly as found in simulations (see Supplementary Video 9), particle clusters are found to displace, disaggregate and remain in a line behind the moving particle clusters. Both cluster disaggregation and particle redistribution over the surface are incomplete due to the 1D spreading of the particle clusters. The applied rotaphoretic field consists of a field rotating out-of-plane at 20 Hz with an in-plane component B_x of 5 mT and an out-of-plane component B_z of 15 mT. The video was recorded at 500 Hz.

Supplementary References

[48] J. Happel, H. Brenner, *Low Reynolds Number Hydrodynamics*, Kluwer Academic Publishers, The Hague, The Netherlands **1983**.